Available online at www.sciencedirect.com
SCIENCE DIRECT
Polymer 47 (2006) 4694–4702
polymer
www.elsevier.com/locate/polymer

Poly(3,4-ethylenedioxythiophene) doped with a non-extrudable metallacarborane anion electroactive during synthesis

Vasile David, Clara Viñas, Francesc Teixidor *

Institut de Ciència dels Materials de Barcelona (CSIC), Campus UAB, 08193 Bellaterra, Spain

Received 25 November 2005; received in revised form 4 April 2006; accepted 4 April 2006
Available online 16 May 2006

Abstract

The electrochemical polymerization of EDOT on ITO from cesium cobaltabisdicarbollide acetonitrile solutions is accompanied by a reversible oxidation of the doping anion. It results in a p-doped polymer embedded with short-chain reduced oligomers, as proven by the material composition, morphology, electrochemical and spectroelectrochemical behaviour. The ratio between the number of EDOT molecules entrapped in the polymer vs. the oligomers is 0.88. This ratio was estimated from the doping level of the material considering that only the polymer can be doped. Its oxidation/reduction process takes place reversibly in the potential range $-0.8/+0.7$ V vs. SCE and is accompanied by cation exchange. The non-extrudable character of the doping anion was proven by electrochemical treatments designed to alter the material composition by ionic exchange followed by EDX or MALDI-TOF mass spectrometric analyses either of the material or of the 0.1 M $LiClO_4$ acetonitrile solution in which the polymer oxidation/reduction had been performed.

Keywords: PEDOT; Cobaltabisdicarbollide; Immobile doppant

1. Introduction

Among the conjugated polymers, CPs, poly(3,4-ethylenedioxythiophene), or PEDOT (see the starting monomer 3,4-ethylenedioxythiophene, EDOT, in Scheme 1), displays a high regularity of the polymeric chain due to the lack of α–β linkages between the monomers, a high stability of the p-doped state and a high conductivity [1,2]. Most of its applications rely on the use of PEDOT polystyrenesulfonate [1]. This material was used recently as a component for electrochromic devices [3], disposable electrodes [4], light emitting diodes [5], electronic memories [6], super capacitors [7], electronic [8] or electrochemical logic circuits [9]. On the other hand, the metallacarborane cobaltabisdicarbollide ($[3,3'\text{-}Co(1,2\text{-}C_2B_9H_{11})_2]^-$, $\mathbf{1}^-$—Scheme 1) has interesting features as a doping agent: a regular peanut shape, a weakly-coordinating ability, a large volume, a low charge density and hydrophobicity [10]. These electronic and structural characteristics have permitted to get polypyrrole materials in which the anion is non-extrudable [10–15], thence resulting in a substantial improvement of the overoxidation resistance [10,11], in selective cation-exchange properties [12], in sensors with a Nernstian response to pH [13,14] and in microcrystalline layers at the polymer surface [15]. Additionally, $\mathbf{1}^-$ experiences a Co(IV)/Co(III) redox-state interconversion [16] at the experimental conditions of EDOT polymerization. The electrochemical doping of CPs with anions electroactive during polymer synthesis may produce innovative materials. Herein, we report the electrochemical synthesis on ITO substrate of PEDOT doped with $\mathbf{1}^-$, PEDOT/$\mathbf{1}^-$, as well as the morphology, doping level, electrochemical and spectroelectrochemical behaviour of the obtained material. In addition, we prove by two original methods (EDX and MALDI-TOF mass spectrometry) the immobility of the doping agent during the polymer switch between the neutral and the p-doped states; it is also shown that an important oligomeric fraction is embedded in the main polymer.

2. Experimental

2.1. Materials and methods

The following reagents were employed as received: $Cs[Co(C_2B_9H_{11})_2]$ ($Cs[\mathbf{1}^-]$, from Katchem Ltd, Prague) and tetraethylammonium chloride hydrate ($NEt_4Cl\times H_2O$), $AgNO_3$, $LiClO_4$ and ferrocene (all from Aldrich). Acetonitrile

* Corresponding author. Tel.: +34 93 580 18 53; fax: +34 93 580 57 29.
E-mail address: teixidor@icmab.es (F. Teixidor).

0032-3861/$ - see front matter © 2006 Elsevier Ltd. All rights reserved.
doi:10.1016/j.polymer.2006.04.017

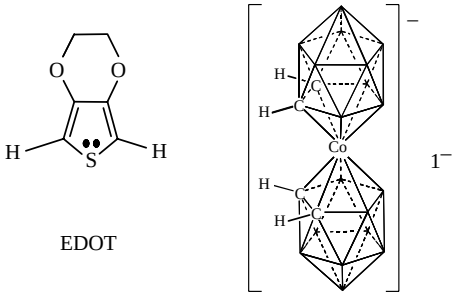

Scheme 1. Structures of the 3,4-ethylenedioxythiophene, EDOT, monomer and of cobaltabisdicarbollide, $[3,3'\text{-}Co(1,2\text{-}C_2B_9H_{11})_2]^-$, $\mathbf{1}^-$. The non-specified vertices in the polyhedral clusters sandwiching the Co moiety in $\mathbf{1}^-$ represent B-H groups.

(from Merck) and EDOT (from Aldrich) were distilled before use.

ITO-covered glass plates (7 mm × 50 mm × 0.7 mm; cat. number: CG-50IN-CUV), with nominal resistance of 8–12 Ω/plate (from Delta Technologies Ltd) were used throughout as working electrodes. The area of the ITO plates kept in contact with the solution was usually of 2 cm^2. A Pt foil (1 cm^2 surface area) or a Pt wire (Φ 0.5 mm, 4 cm) were the counter electrodes employed in the electrochemical syntheses and tests or in the spectroelectrochemical experiments, respectively. The employed reference or pseudoreference electrodes were Ag|AgCl (0.1 M $NEt_4Cl \times H_2O$, acetonitrile) in the electrochemical experiments and $Ag|Ag^+$(10^{-2} M $AgNO_3$, 10^{-1} M $LiClO_4$, acetonitrile) in the spectroelectrochemical tests, respectively. These electrodes were checked with ferrocene solutions in acetonitrile, as recommended by IUPAC [17]. For easy comparison with literature data, the potential values were re-calculated versus SCE using common conversion factors [2]. Therefore, all potential values from the paper are reported with respect to SCE.

A VoltaLab80 (Universal Electrochemical Laboratory System) interfaced with a PGZ402 potentiostat (Radiometer Analytical) and controlled by the VoltaMaster 4 software was used in the electrochemical syntheses as well as in the electrochemical and spectroelectrochemical tests. The absorption spectra of the ITO-supported PEDOT/$\mathbf{1}^-$ (simply, PEDOT/$\mathbf{1}^-$) films and the switch between the neutral and *p*-doped oxidised states (or, simply, the redox switch) were recorded with a PharmaSpec UV-1700 spectrophotometer (Shimadzu) equipped with an 'in situ' spectroelectrochemical cell. SEM images were acquired with a Hitachi S-570 electron microscope, with a beam of 15 keV. The in-depth microchemical analysis of a PEDOT/$\mathbf{1}^-$ film was performed by XPS using a Physical Electronics PHI 5700 spectrometer assisted by argon plasma sputtering and equipped with a non-monochromatic Mg Kα radiation (300 W, 15 kV, 1253.6 eV) as excitation source and with the PHI ACCESS ESCA-V6.0 F software package. Other details related to the XPS analysis can be found elsewhere [18]. The energy dispersive X-ray analysis, EDX, was performed with a JSM-6300 Scanning Electron Microscope (JEOL, Cambridge, UK). MALDI-TOF mass spectra were recorded using the Bruker Biflex instrument [N_2 laser, $\lambda_{ex.}$ 337 nm (0.5 ns pulses); voltage ion source 20.00 kV (Uis1) and 17.50 kV (Uis2)]. The isotope pattern calculation (IPC) was carried out with the Sheffield ChemPuter IPC software from the web address: http://www.chem.shef.ac.uk.

2.2. Procedures

All determinations were performed at ambient temperature (23 ± 2 °C). PEDOT/$\mathbf{1}^-$ films were synthesized galvanostatically in a classical three electrodes, one compartment electrochemical cell from a 0.1 M Cs[$\mathbf{1}^-$], 0.01 M EDOT acetonitrile electropolymerization solution. Unless stated otherwise, the parameters used were a 0.5 mA × cm^{-2} current density and a 200 mC × cm^{-2} electropolymerization charge density, $\sigma_{e,pol}$. The potentiodynamic technique with ohmic drop compensation was also explored to gain additional information about the polymerization mechanism. Only in this case, the area of the ITO surface exposed to the solution was 0.1 cm^2. In addition, a 100 mV × s^{-1} scan rate was employed in this experiment and in the other tests or electrochemical treatments performed by cyclic voltammetry. Before the syntheses, the electropolymerization solutions were purged with dried nitrogen for 10 min.

Immediately after syntheses, the PEDOT/$\mathbf{1}^-$ films for electrochemical or spectroelectrochemical tests were thoroughly washed with anhydrous acetonitrile and then transferred to a 0.1 M $LiClO_4$ acetonitrile solution (referred as electrolyte solution). In the latter, the films were kept for 2 h before being subjected, in new electrolyte solutions, to the subsequent tests. The films devoted to the XPS in-depth microanalysis or to SEM investigations were washed with acetonitrile, dried with purified nitrogen and then kept in the air for maximum 2 days.

To prove the immobility of $\mathbf{1}^-$ during the redox switch, two different procedures were employed. First, five PEDOT/$\mathbf{1}^-$ films were identically prepared, washed with acetonitrile and kept in the electrolyte solution like the films for the electrochemical tests. Next, four of these films were successively transferred to a new electrolyte solution and subjected to different electrochemical treatments consisting in 20 potential scans carried out at different potential ranges and/or with different potential values of start, as shown in Section 3.4. Finally, the film of reference (with no electrochemical treatment) and the other four were washed with acetonitrile, dried with nitrogen and analyzed by EDX. In the second procedure, a 200 mC × m^{-2} PEDOT/$\mathbf{1}^-$ film washed with acetonitrile and kept for 2 h in the electrolyte solution was subjected under stirring to 20 potential scans over the range +0.7/−0.8 V in 10 mL of a new electrolyte solution. Then, the resulting sample solution was analyzed by MALDI-TOF mass spectrometry.

3. Results

3.1. Electrochemical synthesis of PEDOT/$\mathbf{1}^-$

PEDOT/$\mathbf{1}^-$ was synthesized from electropolymerization solutions prepared in anhydrous acetonitrile in which both

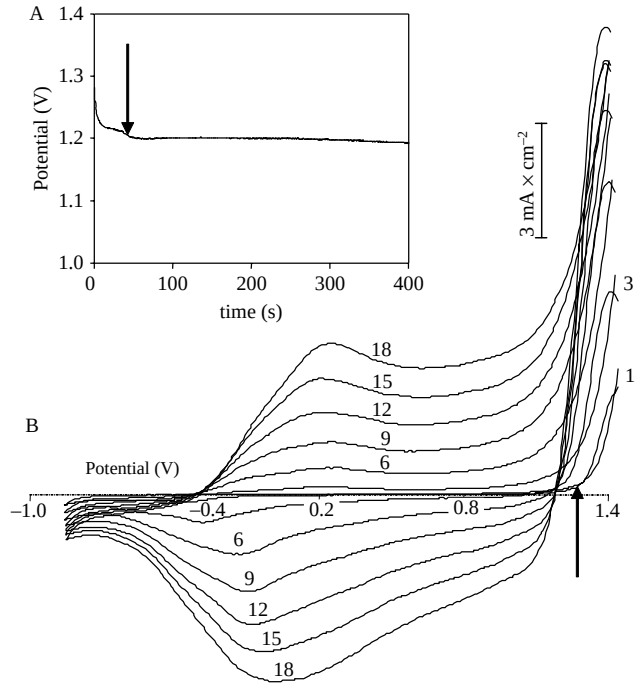

Fig. 1. (A) Potential variation during galvanostatic synthesis of PEDOT/$\mathbf{1}^-$. (B) Potentio-dynamic formation of PEDOT/$\mathbf{1}^-$ on ITO. Cycles 1, 3, 6, 9, 12, 15 and 18 are presented. Except for cycles 1 and 3, the corresponding numbers are written above the curves. In each cycle, the cathodic scans preceded the anodic ones.

EDOT and Cs[$\mathbf{1}^-$] are soluble. A potentiogram recorded during the galvanostatic synthesis of 200 mC × cm^{-2} PEDOT/$\mathbf{1}^-$ is presented in Fig. 1(A). A rapid decay of potential from +1.28 to +1.23 V follows the charging of the double layer and, at about 50 s from the polymerization beginning, the potential definitively stabilizes at +1.20 V (see the vertical arrow in Fig. 1(A)).

Seven voltammograms recorded during the potentiodynamic synthesis of PEDOT/$\mathbf{1}^-$ are presented in Fig. 1(B). As one can see, the electrochemical reactions leading to the polymer formation occur between +0.9 and +1.4 V and the onset of the monomer oxidation is encountered at +1.22 V (see the vertical arrow on the anodic scan from the first cycle in Fig. 1(B)). Current maxima are encountered near +1.36 V on the cathodic scans recorded in the cycles 3–18 which increase until the cycle number 9. This behavior suggests changes during time in the electropolymerization mechanism.

Between +0.6 and +0.9 V, the previously formed polymer is found in highly oxidised state. Nevertheless, high and relatively constant capacitive currents are now recorded due to the quasi-metallic state appearing in the highly doped CPs [19]. One notes that, in the first cycle, the anodic currents from this range are higher in magnitude than the corresponding cathodic ones, which are recorded first.

The oxidation/reduction of the polymer takes place between −0.7 and +0.6 V. The peak potential of polymer oxidation is found at about +0.23 V in all cycles while the reduction peak potential shifts continuously between −0.32 V (nucleation wave) [20] in the first cycle and −0.01 V in the last one.

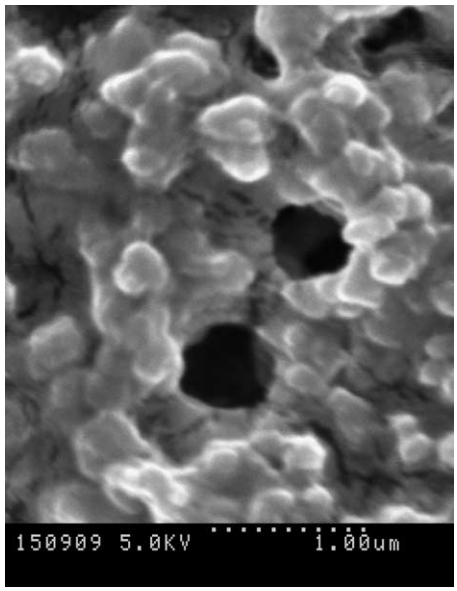

Fig. 2. SEM image of a 50 mC × cm^{-2} PEDOT/$\mathbf{1}^-$ film.

Finally, a rather constant current is recorded in the interval −0.9/−0.7 V, with its magnitude depending linearly on the amount of polymer on the electrode. This current is not due to a reducing character of PEDOT/$\mathbf{1}^-$ because catalytic properties would then be observed, and this was not the case.

3.2. Morphology and elemental composition of PEDOT/$\mathbf{1}^-$

Fig. 2 shows a SEM image of PEDOT/$\mathbf{1}^-$. It reveals networks of interpenetrating globules with few but large pores (up to 0.5 μm diameters). This morphology, that was found to be independent on $\sigma_{e.pol.}$ over the tested range 50–200 mC × cm^{-2}, is characteristic of an amorphous material. It is not in agreement with a two-dimensional kinetics of the polymer growth, as found by Chevrot et al. for PEDOT/ClO_4^- [21].

The XPS microanalysis with argon plasma sputtering proved the in-depth composition homogeneity of a 200 mC × cm^{-2} PEDOT/$\mathbf{1}^-$ film until In and Sn from the support were identified. In atomic percents, the relative composition is: C 53.9%; O 16.2%; S 8.3%; B 20.4% and Co 1.2%. Neither Cs nor N were observed indicating that a significant entrapment followed by a strong bounding in the material of Cs^+ cations or of acetonitrile molecules does not occur during the galvanostatic synthesis.

Considering that the overall electropolymerization reaction is the one presented in Scheme 2, the found composition indicates the low doping level $\gamma = 0.14$. In comparison, the usual doping level of common PEDOTs and polythiophenes is 0.30 [21,22] but a similar doping level to this encountered here was also reported, with no explanation, by Inganäs et al. for PEDOT/Tosylate prepared electrochemically [23].

3.3. Electrochemical and spectroelectrochemical properties

These properties of PEDOT/$\mathbf{1}^-$ were investigated in the optically transparent 0.1 M $LiClO_4$ acetonitrile solution.

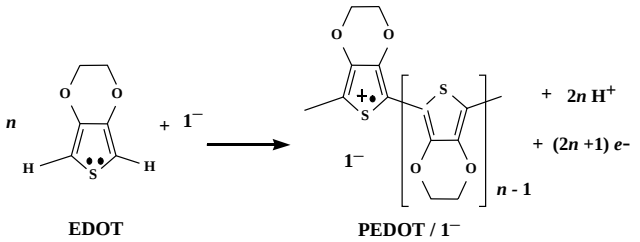

Scheme 2. The overall electropolymerization reaction. The positive charge corresponding to one monomer unit in the polymer ($1/n$) represents the doping level, γ [21].

In a preliminary study, the potential range in which the redox switch of PEDOT/$\mathbf{1}^-$ is reversible was found by cyclic voltammetry to be $-0.8/+0.7$ V in the studied electrolyte. Four voltammograms recorded in this potential range for PEDOT/$\mathbf{1}^-$ films prepared with different $\sigma_{e.pol.}$ are presented in Fig. 3. Only small shifts are noted for the positions of the anodic and cathodic peak potentials with increasing $\sigma_{e.pol.}$ but significant reducing currents are present on the cathodic scans, even at -0.8 V.

The switching charge density, $\sigma_{sw.}$, was computed for each PEDOT/$\mathbf{1}^-$ film by integrating the anodic branches of the voltammograms between -0.4 and $+0.7$ V [21]. As one can see inside Fig. 3, $\sigma_{sw.}$ varies linearly on $\sigma_{e.pol.}$ but the intercept of the regression line differs significantly from zero. However, one concludes that the ionic exchange takes place uniformly in PEDOT/$\mathbf{1}^-$ films with different thicknesses and, from the slope of the regression line, an ion exchange capacity of 5.6 mC$\times$cm^{-2}/(100 mC$\times$cm^{-2} $\sigma_{e.pol.}$) is obtained, in good agreement with the found doping level. Indeed, a charge density of 6.5 mC$\times$cm^{-2}/(100 mC$\times$cm^{-2} $\sigma_{e.pol.}$) is necessary to completely reduce, up to $\gamma=0$, a CP with $\gamma=0.14$. The difference might be due either to an incomplete reduction of

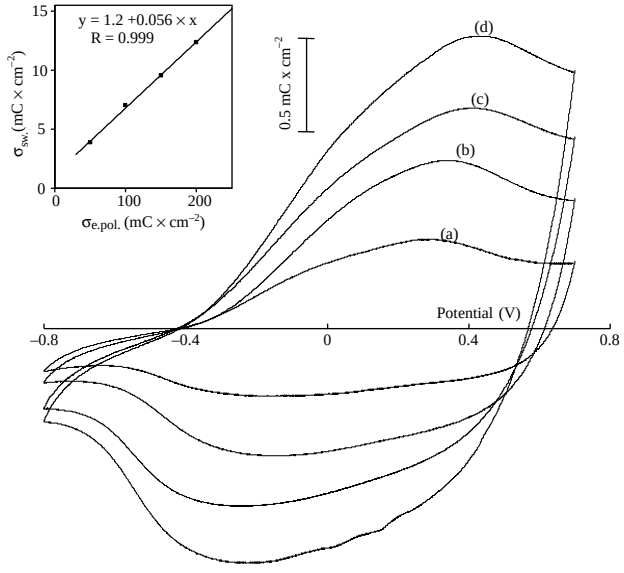

Fig. 3. Voltammograms recorded in 0.1 M $LiClO_4$ acetonitrile solution for PEDOT/$\mathbf{1}^-$ films prepared with the following $\sigma_{e.pol.}$: (a)50; (b)100; (c)150; and (d)200 mC$\times$cm^{-2}. On the left corner, the dependence $\sigma_{sw.}$—$\sigma_{e.pol.}$ is presented.

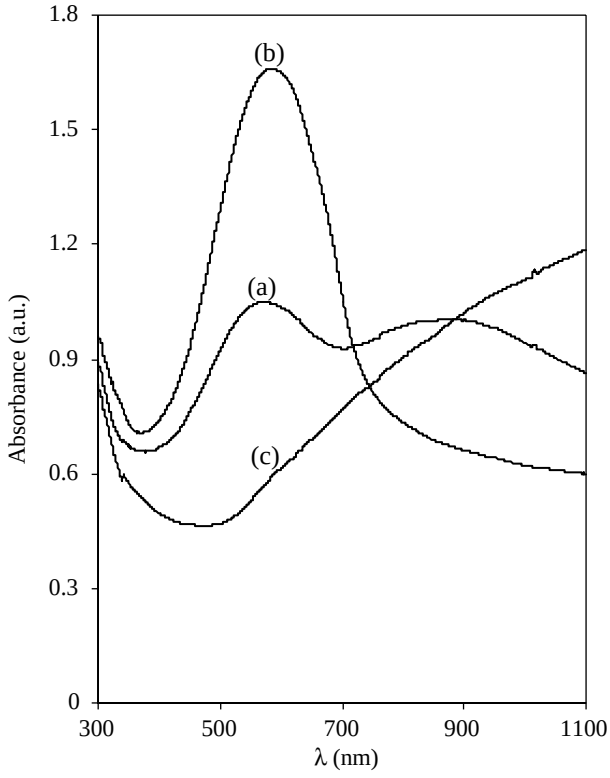

Fig. 4. Absorption spectra acquired from the electrolyte solution for a 200 mC$\times$cm^{-2} PEDOT/$\mathbf{1}^-$ film at the following potentials: (a) OCP (around 0 V); (b) -0.8 V; and (c) $+0.7$ V, respectively.

the PEDOT/$\mathbf{1}^-$, that should be in agreement with other literature data [24], or to a consumption of a part of $\sigma_{e.pol.}$ for producing oligomers that could remain in the electropolymerization solution.

In the electrolyte solution, PEDOT/$\mathbf{1}^-$ attains spontaneously (about 1 h) a potential (the open circuit potential, OCP) close to the average between the potential limits of the potential range of redox switch. The absorption spectra exhibited by a PEDOT/$\mathbf{1}^-$ film at that potential as well as in the reduced and oxidized states are presented in Fig. 4. The absorption band due to the π–π^* electronic transition (or the E_g transition [1,2,25]) is clearly seen in the spectra (a) and (b), its maximum being located at 575 nm. In comparison, the corresponding absorption maximum is found at 610–620 nm in most PEDOTs [2]. The encountered blue shift indicates a low conjugation length of the formed polymer [2,22]. However, a bandgap of 1.5 eV can be calculated from the onset of the E_g transition, in agreement with the literature data [26].

By oxidation, the intensity of absorption due to the π–π^* electronic transition decreases whereas the absorption at higher wavelengths increases due to the low energy charge carriers that appear in highly doped polymers [27,28]. While the absorption spectrum of the fully oxidised PEDOT/$\mathbf{1}^-$ does not exhibit an absorption maximum in the studied optical range, the spectrum recorded at OCP presents the absorption band due to the E_g transition as well as the absorption band E_{b1} [2,25] with the maximum found at 830 nm. Moreover, within an error of $\pm 10\%$, the absorbance at 575 nm of the PEDOT/$\mathbf{1}^-$ found

at OCP is the arithmetic average of the absorbances at the same wavelength exhibited by the reduced and oxidized states of PEDOT/$\mathbf{1}^-$.

Although a low doping level was found for PEDOT/$\mathbf{1}^-$, the shape of the absorption spectra is similar to that reported by other authors for PEDOTs with an assumed doping level of 0.30 [25,26,29]. Nevertheless, three important differences can be noted in addition to the blue shift mentioned before: an abnormally high absorption exhibited by the oxidised PEDOT/$\mathbf{1}^-$ under 600 nm; an about twice smaller absorbance exhibited by the reduced PEDOT/$\mathbf{1}^-$ at 575 nm by comparison with PEDOT/ClO_4^- prepared at the same $\sigma_{e.pol.}$; and a significant absorption band found at wavelengths smaller than 400 nm, whose tail is observed for all three PEDOT/$\mathbf{1}^-$ states. As it will be shown in Section 4, they are the consequences of the PEDOT/$\mathbf{1}^-$ forming conditions.

The stability of the PEDOT/$\mathbf{1}^-$ to repetitive redox switches and the switching time were studied by monitoring at 575 nm the absorbance variation during the time in which a PEDOT/$\mathbf{1}^-$ film was alternatively impressed with potentials of −0.8 and +0.7 V, respectively. The results obtained during the first 20 switches are presented in Fig. 5. As it can be seen, no significant modification is noted in the amplitude of the absorbance variation. The same trend is observed for at least 100 switches between −0.8 and +0.7 V. The switching time [2], of near 5 s, is of the same order of magnitude with that reported by Inganäs et al. in a solid state electrochromic cell [29].

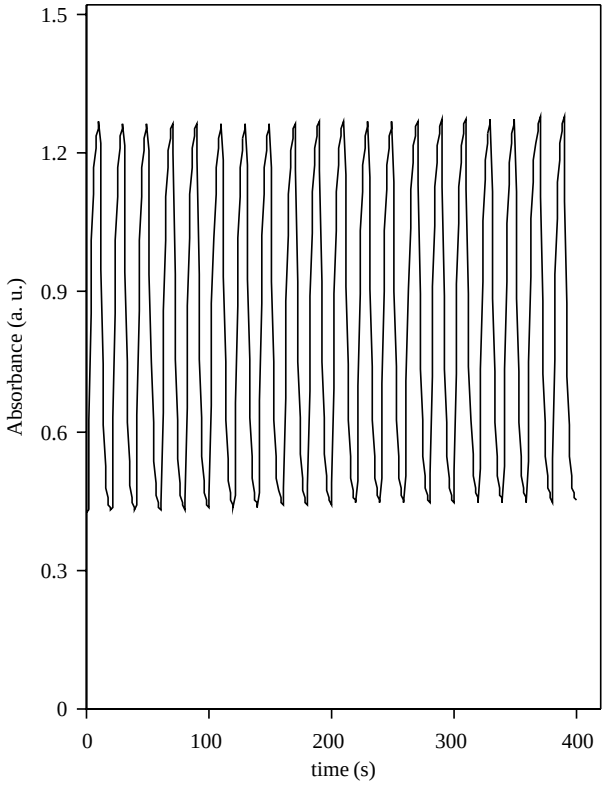

Fig. 5. Variation on time of the absorbance at 575 nm for a 200 mC×cm^{-2} PEDOT/$\mathbf{1}^-$ film during repetitive changes of potential between −0.8 V (10 s) and +0.7 V (10 s), respectively.

3.4. Immobility of $\mathbf{1}^-$ during the polymer oxidation/reduction

Because the voltammograms obtained in the potentiodynamic synthesis of PEDOT/$\mathbf{1}^-$ do not furnish enough information about the nature of the ion(s) exchanged during the polymer oxidation/reduction, the procedures described in Section 2.2 were used to test the mobility of $\mathbf{1}^-$ during the redox switch. Fig. 6 summarizes the results obtained in the EDX analysis of five PEDOT/$\mathbf{1}^-$ films subjected to electrochemical treatments designed to alter differently the PEDOT/$\mathbf{1}^-$ composition by ionic exchange (see also Section 2.2). In all cases, the same Co:S ratio as the one found by XPS was obtained, indicating that $\mathbf{1}^-$ had not been replaced by ClO_4^- in any of the electrochemical treatments.

The low coordinating ability of $\mathbf{1}^-$ [10] and the low dissociation in acetonitrile of the $LiClO_4$ salt [30] prompted us to assess the MALDI-TOF mass spectrometric analysis of traces of $\mathbf{1}^-$ in 0.1 M $LiClO_4$ acetonitrile solutions. If $\mathbf{1}^-$ in PEDOT/$\mathbf{1}^-$ would be mobile, then it would be replaced significantly by ClO_4^- during 20 redox switches. In such a case, a $\mathbf{1}^-$ concentration of the order of 10^{-5} M would be present in the sample solution obtained as described in Section 2.2 [31]. The mass spectra of the sample solution (see Section 2.2) and of a reference solution containing both Cs[$\mathbf{1}^-$] and $LiClO_4$ in a 10^{-4} molar ratio are presented in Fig. 7. In the optimum m/z range selected for work, the spectrum of the sample solution exhibits only the isotopic peaks characteristic of the perchlorate ionic association $[Li(ClO_4)_2]^-$ while the one of the reference solution displays also the peak group of $\mathbf{1}^-$, as proven by the isotopic patterns. In these conditions, the lack of the peak group centered at $m/z=324$ in the spectrum of the sample solution, further sustains the non-extrudability of $\mathbf{1}^-$ during the redox switch.

4. Discussion

As already shown in Section 3, the properties of PEDOT/$\mathbf{1}^-$ are rather different from those of other PEDOT polymers doped electrochemically with mobile anions. Main differences consist in the proven morphology, in the doping level, in the low ratio between the absorption of the reduced state and $\sigma_{e.pol.}$, in the blue shift of the main absorption maximum, and in the apparent reducing character of PEDOT/$\mathbf{1}^-$. In addition, the immobility of $\mathbf{1}^-$ during the redox switch results in a narrow potential range of redox switch. This property might result in important practical applications and will be detailed in a future paper.

Most differences between the properties of PEDOT/$\mathbf{1}^-$ and of common PEDOTs reside in the formation particularities of PEDOT/$\mathbf{1}^-$ which evolve from the electroactivity of $\mathbf{1}^-$ during the galvanostatic and potentiodynamic syntheses. Indeed, in a complementary study (see Appendix A), we found that the following equilibrium takes place in similar conditions to those employed for PEDOT/$\mathbf{1}^-$ syntheses:

$$\underset{\mathbf{1}^-}{[Co(C_2B_9H_{11})_2]^-} \rightleftharpoons \underset{\mathbf{1}^0}{[Co(C_2B_9H_{11})_2]_{ads}} + e^- \qquad E_{1/2} \approx +1.26\ V$$

where $\mathbf{1}^0$ adsorbs on ITO. The half wave potential of this equilibrium, $E_{1/2}$, is lower than the irreversible oxidation

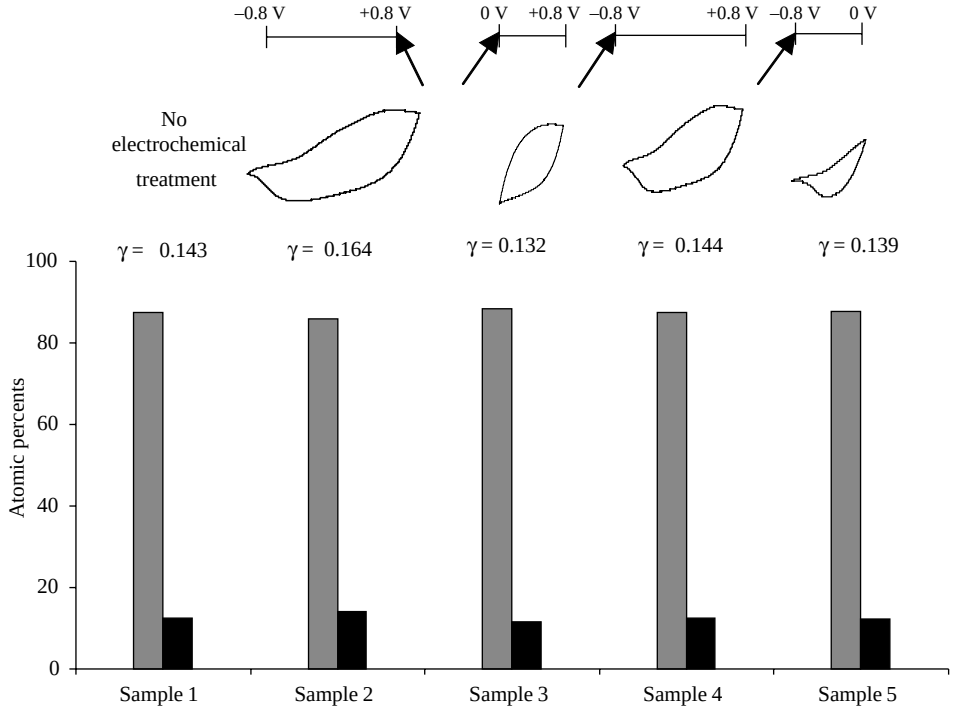

Fig. 6. Relative atomic percents found for S (grey rectangles) and for Co (black rectangles) by EDX microanalysis in five PEDOT/$\mathbf{1}^-$ samples subjected to potential scans in the ranges presented in the upper part of the figure, as detailed in Section 2.2. The starting potentials are indicated by arrows at one end of the potential ranges and, below these, the shape of the voltammograms is presented. The doping levels with $\mathbf{1}^-$ of the different PEDOT/$\mathbf{1}^-$ samples (or, equivalently, the Co:S ratio, γ) are also included between the histograms and the electrochemical treatments.

potential of EDOT (about +1.4 V) [2,21,25] but it is similar to the potentials recorded during our galvanostatic syntheses (see Fig. 1(A)). Consequently, a concurrent oxidation of $\mathbf{1}^-$ and EDOT occurs during the electrochemical syntheses of PEDOT/$\mathbf{1}^-$. This implies that a competition for the electrodic surface of the two species takes place. Nevertheless, the most part of $\sigma_{e.pol.}$ is consumed in the reaction from Scheme 2, where the formed polymer and oligomers are found either deposited onto the electrode or solved in solution. It is because $\mathbf{1}^0$ will be finally reduced to $\mathbf{1}^-$ by electron capture either from the

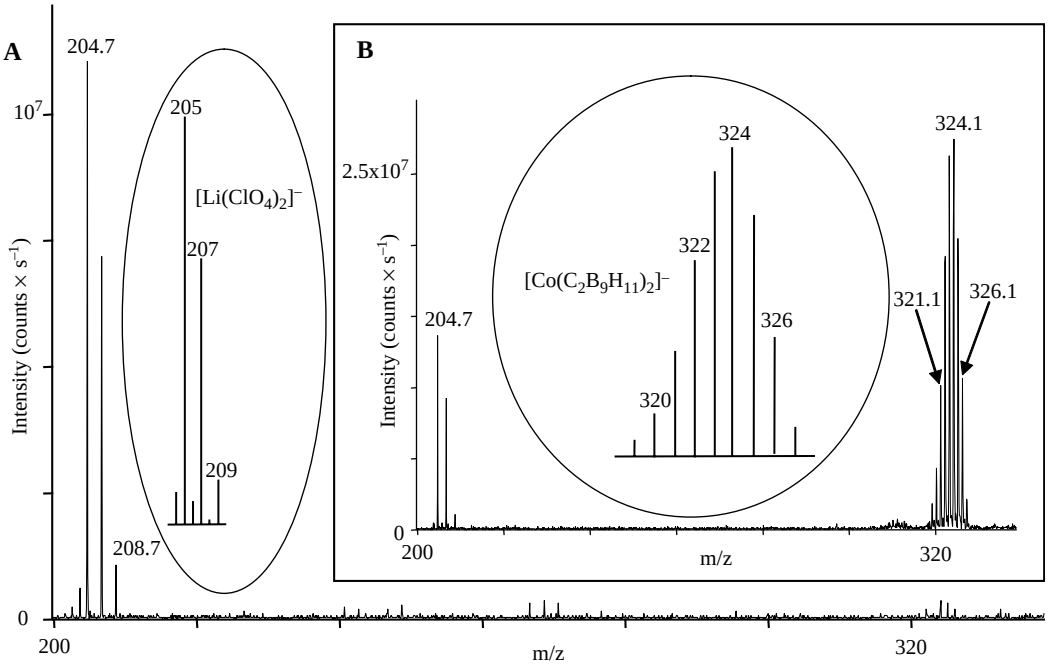

Fig. 7. MALDI-TOF mass spectra for: (A) sample solution (see Section 2.2); and (B) 0.1 M $LiClO_4$ and 10^{-5} M Cs[$\mathbf{1}^-$] acetonitrile reference solution, respectively. The isotopic patterns of $[Li(ClO_4)_2]^-$ and of $\mathbf{1}^-$ are also included near the corresponding peak groups.

electrode bulk or from the EDOT molecules found near the electrode before being entrapped into the polymer as doping anion or being escaped into the solution. In whatever case, the current due to the $\mathbf{1}^-$ oxidation is annihilated. In such conditions, the conclusions derived in Section 3 from the values of $\sigma_{e.pol.}$ must be correct.

The adsorption on ITO of $\mathbf{1}^0$ could hinder the layer-by-layer growth [21] of the polymer and, thus, it might determine the encountered morphology (see Fig. 2). Moreover, this process is more important in the first synthesis stages and this fact might explain the potential decay in the system at about 50 s from the beginning of the galvanostatic synthesis (see Fig. 1(A)). The more cathodic location of the reduction peak from the voltammograms recorded in the first cycle of the potentiodynamic syntheses is explained as follows. At high potentials, short-chain, positively-charged oligomers are formed initially in the solution adjacent to the electrode surface from $EDOT^+$ and EDOT. Due to the $\mathbf{1}^0$ adsorption on ITO, those oligomers cannot nucleate on the electrode surface at the potentials at which they are formed but it will happen at relatively cathodic potentials where the electrode surface is charged negatively enough to exhibit a sufficient electrostatic attraction of the oligomers. This interpretation is also sustained by the ratio between the anodic and cathodic capacitive currents recorded in the first cycle between +0.6 and +0.9 V (see Fig. 1(B)), which clearly proves that the polymer forms at the electrode surface in the time interval elapsed between their acquisitions.

After the nucleation took place in whatever variant of electrochemical synthesis, the oligomers from solution either might be incorporated into the polymer chain, either might remain in the solution, or might be simply entrapped in the material. Whereas the analysis after the synthesis of the electropolymerization solution indicated low levels of oligomers (data not shown), the properties of the material and the literature data sustain the massive incorporation of the latter into PEDOT/$\mathbf{1}^-$. Indeed, it is known that bis-EDOT [32] and ter-EDOT [33] are monomers less reactive than EDOT, then giving rise by electropolymerization to polymers having the absorption maxima highly blue-shifted [2,32,33]. In our case, the oligomers might be responsible of the absorption band seen in the spectra at wavelengths lower than 400 nm (see Fig. 4). This band resembles more the π–π* absorption band of EDOT than the one of PEDOT and, therefore, it sustains the entrapment of oligomers into PEDOT/$\mathbf{1}^-$.

The ionic exchange capacity and the absorbance values of PEDOT/$\mathbf{1}^-$ in reduced state (which is about twice lower than for PEDOT/ClO_4^- [26]) agree well with the found doping level. They also sustain the hypothesis that PEDOT/$\mathbf{1}^-$ consists of a main polymeric chain, which can be doped up to the theoretical level of $\gamma = 0.30$, and from an un-dopable oligomeric fraction found in the reduced state. The ratio between the number of EDOT monomers entrapped in the polymeric and oligomeric fractions of PEDOT/$\mathbf{1}^-$ is 0.88, as it results from the γ values of 0.30 and 0.14 which are characteristic to the common PEDOTs [21,22] and to the PEDOT/$\mathbf{1}^-$, respectively, [34].

Although the PEDOT/$\mathbf{1}^-$ composition determined by XPS does not exhibit significant in-depth changes, the $\mathbf{1}^0$ adsorption on ITO in the first stage of the electrochemical synthesis might result, near the ITO surface, in a ratio between the polymeric and oligomeric fractions higher than 0.88 and this fact might explain the non-zero intercept of the regression line from Fig. 3.

An intriguing aspect exhibited by PEDOT/$\mathbf{1}^-$ consists in its apparent reducing character. One observes that neither the PEDOT reduction to an *n*-doped state [35], nor the $\mathbf{1}^-$ reduction as a result of a Co(III)/Co(II) interconversion [16] are possible in the −0.9/−0.4 V potential range because these processes occur at potentials more cathodic than −1.85 V [2,35] and −1.42 V [16], respectively. In such conditions, to find the origin of the cathodic currents recorded constantly during the cathodic scans at the most negative potentials explored by us, a PEDOT/$\mathbf{1}^-$ film was polarised continuously at −0.8 V for 1 h in the same electrolyte solution in which the electro- and spectroelectrochemical tests were performed. The MALDI-TOF mass spectrum acquired in positive mode for the resulting solution indicated the presence of short-chain oligomers of EDOT (data not shown). Consequently, one considers that a reductive dissolution of the oligomeric fraction takes place at cathodic potentials, representing the source of the long-time instability proven by PEDOT/$\mathbf{1}^-$ to very great numbers of redox switches. Nevertheless, this phenomenon (which simply allow the controlled removal of the oligomeric fraction by means of an electrochemical stimulus) might be useful in some practical applications or theoretical studies, either for the enrichment of the material in the polymeric fraction or for the preparation of very dilute solutions of EDOT oligomers. Such solutions could then be added over analytical samples containing chemical substances with molecular masses spread in the mass range of the oligomers as a unique internal standard in the mass spectrometric determination of all compounds.

5. Conclusions

The use of the voluminous metallacarborane anion cobaltabisdicarbollide for the electrochemical doping of PEDOT on ITO support results in a material with properties very different from those of PEDOT/ClO_4^- concerning both the doping level, the morphology, and the electrochemical and spectroelectrochemical behaviour as well as a specific apparent reducing character. Most of the found differences have the origin in the concurrent oxidation on ITO between the doping anion and EDOT during the synthesis which gives rise to a polymer mixed with short-chain oligomers found in reduced state.

Only the polymer fraction can be p-doped and reversibly undoped in the potential range −0.8/+0.7 V vs. SCE while the oligomeric fraction suffers an irreversible reductive dissolution at potentials lower than −0.4 V vs. SCE. The immobility of the doping anion during the polymer oxidation/reduction was proven by two original procedures relying on electrochemical treatments designed to alter the material composition by ionic exchange followed by EDX or MALDI-TOF mass spectrometric analyses either of the material itself or of the 0.1 M

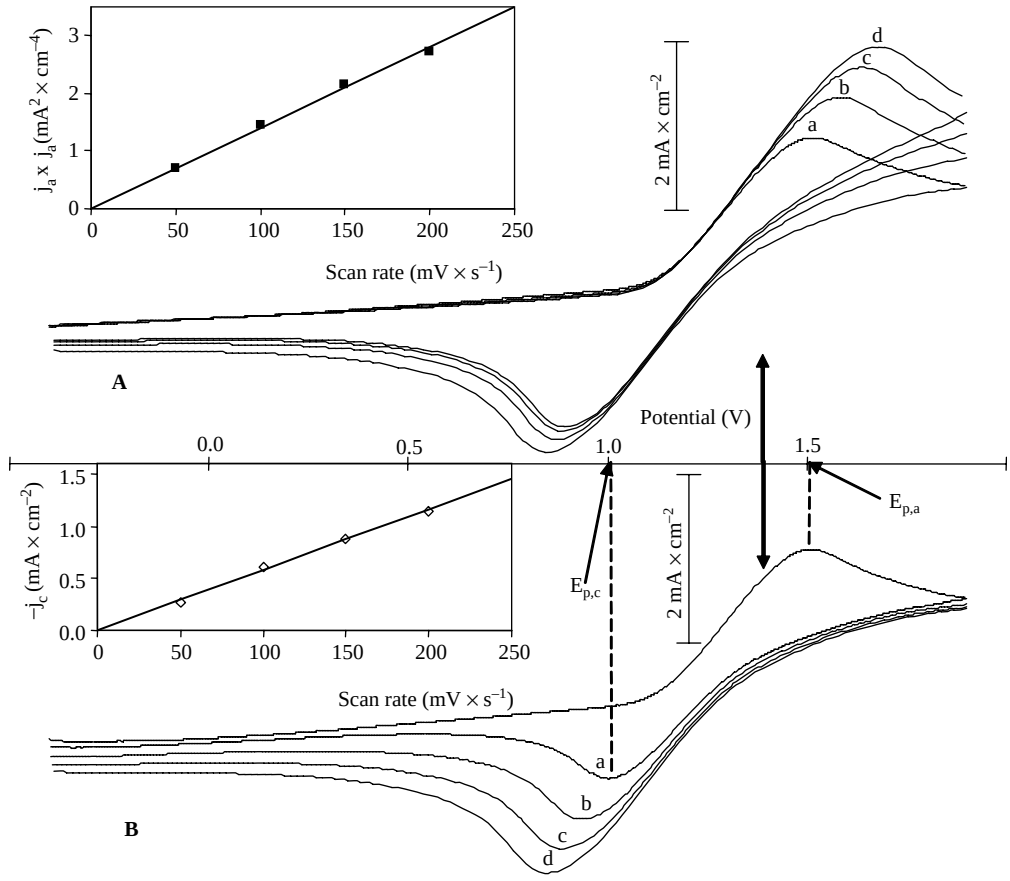

Fig. A1. (A)Voltammograms acquired at the following anodic scan rates: (a) 50; (b) 100; (c) 150 and (d) 200 mV × s^{-1}, respectively. Inside, the dependence on scan rate of j_a^2 is tested. (B) Voltammograms acquired at the following cathodic scan rates: (a) 50; (b) 100; (c) 150 and (d) 200 mV × s^{-1}, respectively. Inside, the dependence on scan rate of $-j_c$ is tested. j_a, j_c—current densities at the anodic or cathodic peaks measured vs. a baseline derived as shown elsewhere [36]; $E_{1/2} = (E_{p,a} + E_{p,c})/2$. See text for other conditions.

$LiClO_4$ acetonitrile solution in which the polymer oxidation/reduction had been performed, repetitively.

Acknowledgements

Support by CICYT (Project MAT2004-01108) and Generalitat de Catalunya (2001/SGR/00337). V.D. thanks the Ministerio de Educación, Cultura y Deporte for a postdoctoral fellowship.

Appendix A. Electrochemical behaviour of cobaltabisdicarbollide on ITO

The electrochemical behaviour of $\mathbf{1}^-$ on ITO was studied by Cyclic Voltammetry from a 0.01 M Cs[$\mathbf{1}^-$], 0.1 M $LiClO_4$ acetonitrile test solution. The investigated potential range, whereby the supporting electrolyte ($LiClO_4$) is electrochemically inactive was $-0.4/+1.9$ V.

The voltammograms acquired with variable anodic scan rates but with the same cathodic scan rate (200 mV × s^{-1}) or with a 50 mV × s^{-1} anodic scan rate but with variable cathodic scan rates are presented in Fig. A1 (A and B, respectively). In the second case, the same amount of electroactive species was oxidized every time during the anodic scan. A quasi-reversible redox process is observed. Its half wave potential, $E_{1/2} = +1.26$ V, is estimated from the positions of the anodic and cathodic peaks in the voltammogram recorded with scan rates of 50 mV × s^{-1} in both directions ($E_{p,a} = +1.51$ V; $E_{p,c} = +1.01$ V; see Fig. A1(B)).

The variation of the voltammograms shape on scan rate indicates that the anodic and cathodic waves are due to the oxidation of a chemical species from solution and to the reduction of a chemical species adsorbed onto the electrode surface, respectively, [36].

References

[1] Groenendaal BL, Jonas F, Freitag D, Pielartzik H, Reynolds JR. Adv Mater 2000;12(12):481–94.
[2] Groenendaal BL, Zotti G, Aubert PH, Waybright SM, Reynolds JR. Adv Mater 2003;15(11):855–79.
[3] Argun AA, Cirpan A, Reynolds JR. Adv Mater 2003;15(16):1338–41.
[4] Michalska A, Ocypa M, Maksymiuk K. Electroanalysis 2005;17(4):327–33.
[5] Ma WL, Iyer PK, Gong X, Liu B, Moses D, Bazan GC, et al. Adv Mater 2005;17(3):274–7.
[6] Möler S, Perlov C, Jackson W, Taussing C, Forrest S. Nature 2003;426(6963):166–9.
[7] Li WK, Chen J, Zhao JJ, Zhang JR, Zhu JJ. Mater Lett 2005;59(7):800–3.

[8] Liu YX, Cui TH. Solid State Electron 2005;49(3):445–8.
[9] Nilsson D, Robinson D, Berggren M, Forchheimer R. Adv Mater 2005; 17(3):353–8.
[10] Masalles C, Borros S, Viñas C, Teixidor F. Adv Mater 2000;12(16): 1199–2002.
[11] Masalles C, Llop J, Viñas C, Teixidor F. Adv Mater 2002;14(11):826–9.
[12] Masalles C, Borros S, Viñas C, Teixdor F. J Organomet Chem 2002; 657(1–2):239–46.
[13] Zine N, Bausells J, Ivorra A, Aguilo J, Zabala M, Teixidor F, et al. Sens Actuat B 2003;91(1–3):76–82.
[14] Masalles C, Borros S, Viñas C, Teixidor F. Anal Bioanal Chem 2002; 372(4):513–8.
[15] Masalles C, Borros S, Viñas C, Teixidor F. Adv Mater 2002;14(6): 449–52.
[16] Hawthorne MF, Young DC, Andrews TD, Howe DH, Pilling RL, Pitts AD, et al. J Am Chem Soc 1968;90(4):879–96.
[17] Gritzner G, Kuta J. Pure Appl Chem 1984;56(4):461–6.
[18] Hernán L, Morales J, Sánchez L, Santos J. Rodríguez Castellón E. Solid State Ionics 2000;133(1–3):179–88.
[19] Feldberg SW. J Am Chem Soc 1984;106(17):4671–4.
[20] Asavapiriyanont S, Chandler GK, Gunawardena GA, Pletcher D. J Electroanal Chem 1984;177(1–2):245–51.
[21] Randriamahazaka H, Noël V, Chevrot C. J Electroanal Chem 1999; 472(2):103–11.
[22] Nalva HS(Ed). Handbook of Conductive molecules and Polymers, 1–4. New York: Wiley; 1997.
[23] Xing KZ, Fahlman M, Chen XW, Inganäs O, Salaneck WR. Synth Met 1997;89(3):161–5.
[24] Zykwinska A, Domagala W, Czardybon A, Pilawa B, Lapkowski M. Chem Phys 2003;292(1):31–45.
[25] Dietrich M, Heywang JHG, Jonas F. J Electroanal Chem 1994;369(1-2): 87–92.
[26] Pei Q, Zuccarello G, Ahlskog M, Inganäs O. Polymer 1994;35(7): 1347–51.
[27] van Haare JAEH, Havinga EE, van Dongen JLJ, Janssen RAJ, Cornil J, Brédas J-L. Chem Eur J 1998;4(8):1509–22.
[28] Zykwinska A, Domagala W, Pilawa B, Lapkowski M. Electrochimica Acta 2005;50(7–8):1625–33.
[29] Gustafsson JC, Liedberg B, Inganäs O. Solid State Ionics 1994;69(2): 145–52.
[30] Gurunathan K, Murugan AV, Marimuthu R, Mulik UP, Amalnerkar DP. Mater Chem Phys 1999;61(3):173–91.
[31] Indeed, because a PEDOT/$\mathbf{1}^-$ film with a 2 cm^2 area and with an ionic exchange capacity of 12.4 mC cm^{-2} (obtained from the regression line presented in Fig. 3) was subjected at 20 redox switches in 10 mL electrolyte solution, around 2.57×10^{-7} mol of $\mathbf{1}^-$ would be released in the sample solution (i.e. 2 $cm^2\times12.4$ mC cm^{-2}/96,500 C $mole^{-1}$) if $\mathbf{1}^-$ would be replaced totally by ClO_4^-. It would produce a 2.57×10^{-5} M concentration of $\mathbf{1}^-$ in the sample solution (2.57×10^{-7} mol/0.01 L solution).
[32] Sötzing GA, Reynolds JR, Steel PJ. Adv Mater 1997;9(10):795–8.
[33] Sötzing GA, Reynolds JR, Steel PJ. Chem Mater 1996;8(4):882–9.
[34] Doping ratios in PEDOT/$\mathbf{1}^-$ and in normal PEDOTs are 7.14 and 3.33, respectively. Then, 2.14 (i.e.: 7.14/3.33) represents the ratio between the total amount of S from PEDOT/$\mathbf{1}^-$ and the amount found in the polymeric fraction. Finally, 0.88 (or 1/(2.14-1)) will represent the ratio between the amounts of S found in the polymeric and oligomeric fractions.
[35] Ahonen HJ, Lukkari J, Kankare J. Macromolecules 2000;33(18): 6787–93.
[36] Brett CMA, Brett AMO. Electrochemistry. Principles, methods, and applications, vol. 9. Oxford: Oxford University Press; 1993 (chapter 9).